

编号: 0258-7106(2011)02-0339-10

西藏甲玛中酸性侵入岩 LA-ICP-MS 锆石 U-Pb 定年及成矿意义*

秦志鹏¹, 汪雄武¹, 多吉^{1,2}, 唐晓倩¹, 周云¹, 彭惠娟¹

(1 成都理工大学, 四川 成都 610059; 2 西藏自治区地质矿产勘查开发局, 西藏 拉萨 851400)

摘要 文章研究了甲玛矿区中酸性侵入岩的侵位时序及岩浆-成矿作用。以实测地质资料为基础, 结合中酸性侵入岩的 LA-ICP-MS 锆石 U-Pb 定年, 初步厘定了甲玛矿区中酸性岩浆岩的侵位时序, 从早到晚依次为: 花岗斑岩(15.31~16.27 Ma)—石英闪长玢岩—二长花岗斑岩(14.81 Ma)—花岗闪长斑岩。以辉钼矿为例, 甲玛矿床显示有 3 期成矿作用, 各期成矿过程分别对应于花岗斑岩或石英闪长玢岩、二长花岗斑岩和花岗闪长斑岩 3 期不同强度的岩浆作用过程。甲玛矿床的形成是 3 期岩浆-成矿作用叠加的结果。

关键词 地球化学; LA-ICP-MS 锆石 U-Pb 定年; 成矿意义; 甲玛; 西藏

中图分类号: P597+.3

文献标志码: A

LA-ICP-MS U-Pb zircon age of intermediate-acidic intrusive rocks in Jiama of Tibet and its metallogenic significance

QIN ZhiPeng¹, WANG XiongWu¹, DOR Ji^{1,2}, TANG XiaoQian¹, ZHOU Yun¹ and PENG HuiJuan¹

(1 Chengdu University of Technology, Chengdu 610059, Sichuan, China; 2 Tibet Bureau of Geology and Mineral Exploration and Development, Lhasa 851400, Tibet, China)

Abstract

This paper deals with the emplacement timing of the intermediate-acidic intrusive rocks in Jiama of Tibet and its metallogenic significance. Based on the measured geological data and LA-ICP-MS U-Pb zircon ages of the four intermediate-acidic intrusive rocks, the authors preliminarily regularized the timing sequence, which is from early to late in order of porphyry granite (15.31 Ma~16.27 Ma)-quartz diorite porphyrite-adamellite porphyry (14.81 Ma)-granodiorite-porphyry; Exemplified by molybdenum, the Jiama ore deposit assumes three periods of metallogenesis, i. e., the ore-forming processes corresponding respectively to different degrees of magmatic activities of porphyry granite or quartz diorite porphyrite, adamellite porphyry and granodiorite-porphyry. The Jiama ore deposit resulted from the superposition of the three periods of magma-mineralization.

Key words: geolcemistry, LA-ICP-MS zircon U-Pb dating, metallogenic significance, Jiama, Tibet

西藏甲玛铜多金属矿床以矽卡岩-角岩型铜钼铅锌(金、银)矿体为主,与驱龙斑岩铜矿毗邻,是冈底斯成矿带东段与斑岩成矿系统有关的最具代表性的超大型铜多金属矿床。矿区内岩浆岩发育,类型

* 本文得到国家 973 项目(编号:2011CB403103)国土资源部科学基地协作研究(编号:200911007-02)青藏专项(编号:1212010818089)技术开发项目(编号:E0804)教育部学科建设项目(编号:SZD0407)的共同资助

第一作者简介 秦志鹏,男,1983年生,在职博士生,矿床学专业。Email: qinyu83@Gmail.com

收稿日期 2010-11-25; 改回日期 2011-02-14。许德焕编辑。

复杂,矽卡岩的形成和成矿作用在时空上与岩浆活动关系密切。其中,二长花岗斑岩和花岗闪长斑岩具埃达克岩的地球化学特征(应立娟等,2009;唐菊兴等,2010)。迄今,对该区各类岩浆岩,尤其是中酸性岩浆岩的侵位时序的厘定还缺少确凿的证据。本文旨在通过对甲玛矿区花岗斑岩及二长花岗斑岩 LA-ICP-MS 锆石 U-Pb 年龄的测定,并结合野外资料,来厘定其成岩作用的演化时序,并划分成矿作用的阶段,以揭示岩浆-成矿作用的关系。

1 矿床地质特征

甲玛铜多金属矿床位于冈底斯成矿带的东段,拉萨地体南缘,冈底斯火山-岩浆弧内,局限产于第三纪 NS 向正断层及裂谷系统(墨竹工卡-错那裂谷)中(Harrsion et al., 1995; Coleman et al., 1995;

Yin et al., 2000)。

该矿区内出露的地层主要为被动陆缘期的碎屑岩-碳酸盐岩系,包括上侏罗统多底沟组、下白垩统林布宗组,以及少量第四系。NW 向褶皱组成的推覆-滑覆构造系形成了该矿区的构造格局。

岩浆岩类型复杂,呈岩株或岩脉产出。岩石类型有花岗斑岩、花岗闪长斑岩、二长花岗斑岩、石英闪长玢岩和辉绿玢岩,以二长花岗斑岩、花岗闪长斑岩为主。岩浆岩产状与区域构造密切相关,花岗斑岩及辉绿玢岩受区域推覆构造的制约,呈近 EW 向产于褶皱的转折端,其长轴方向与构造线及地层走向一致;花岗闪长斑岩、二长花岗斑岩、石英闪长玢岩受区域拉张环境及走滑断层的控制,整体呈 NW-SE 向、近 NS 向的雁列式展布(图 1)。

在矿区范围内,花岗斑岩多被花岗闪长斑岩切穿(图 2A)或被捕虏于石英闪长玢岩内(图 2B);二长

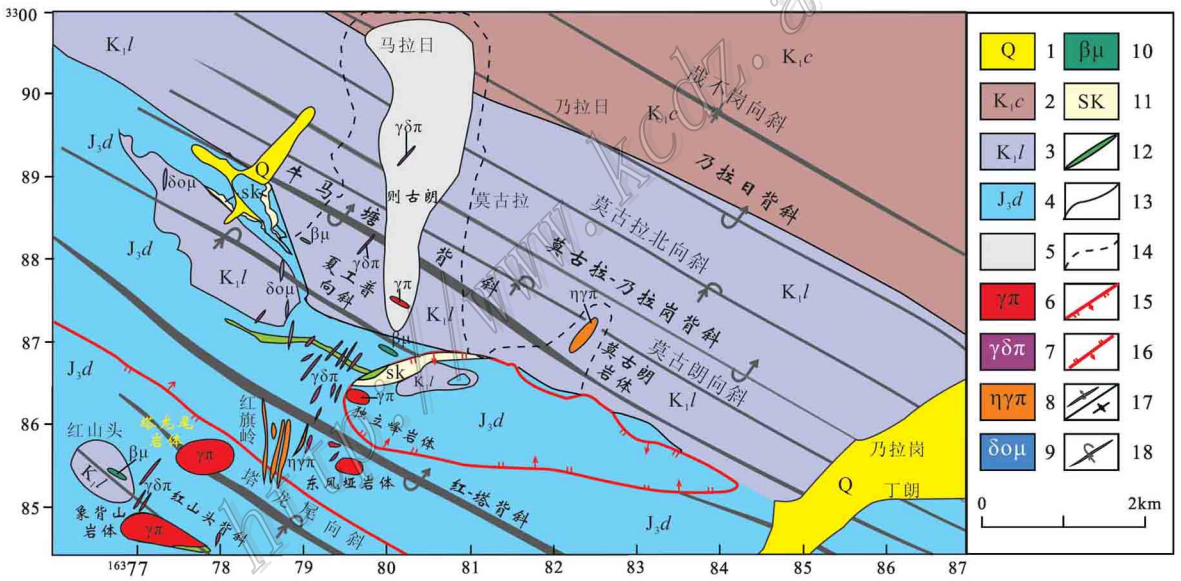


图 1 甲玛矿床构造纲要图

1—第四系; 2—楚木龙组; 3—林布宗组; 4—多底沟组; 5—硅帽; 6—花岗斑岩; 7—花岗闪长斑岩; 8—二长花岗斑岩; 9—石英闪长玢岩; 10—辉绿玢岩; 11—矽卡岩; 12—矿体; 13—地层界线; 14—角岩蚀变界线; 15—正断层; 16—逆断层; 17—斜歪倒转背斜; 18—斜歪倒转向斜

Fig. 1 Tectonic map of the Jiama ore deposit

1—Quaternary; 2—Chumulong Formation (K_{1c}); 3—Linbuzong Formation (K_{1l}); 4—Duodigou Formation (J_{3d}); 5—Silicification zone; 6—Granitic porphyry; 7—Granodioritic porphyry; 8—Monzogranitic porphyry; 9—Quartz-dioritic porphyrite; 10—Diabase-porphyrite; 11—Skarn; 12—Ore body; 13—Stratigraphic boundary; 14—Hornfels alteration boundary; 15—Normal fault; 16—Reversed fault; 17—Inverted anticline; 18—Inverted syncline

唐菊兴,王登红,钟钟惠,汪雄武,郭衍游,刘文周,应立娟,郭娜,郭科,郑文宝,秦志鹏,李磊,凌娟,叶江,黎枫信,姚晓峰,李志军,孙艳,王友,白景国,唐晓倩,张丽,裴有哲,彭惠娟. 2009. 西藏自治区墨竹工卡县甲玛矿区外围铜多金属矿详查报告. 内部资料.

花岗斑岩多含石英闪长玢岩的捕虏体(图 2C), 但被花岗闪长斑岩所切穿(图 2D)。此外, 在花岗斑岩和石英闪长玢岩内均发育不同程度的矽卡岩化(图 2E、F), 而二长花岗斑岩则明显晚于含矿矽卡岩(图 3A)。花岗斑岩、花岗闪长斑岩、二长花岗斑岩和石英闪长玢岩内均发育不同程度的 Cu、Mo 矿化(图 2D、3B、3C), 以花岗斑岩为最。

2 样品特征

本次测试的样品为 3 件花岗斑岩(样品号及取样位置分别为: TLW(X = 16377836, Y = 3285813, Z = 5072), XBS(X = 16377086, Y = 3284944, Z =

5203), DLF(X = 16379542, Y = 3286285, Z = 4778)) 和一件二长花岗斑岩(样品号及取样位置为 DFY(X = 16380052, Y = 3286290, Z = 5066))。样品特征如下:

花岗斑岩 浅灰白色, 斑状结构, 块状构造(图 3D), 斑晶含量约占 50%, 主要矿物组合为石英(60%) + 钾长石(20%) + 斜长石(12%) + 黑云母(6%) + 角闪石(2%)(图 3E), 副矿物组成为磷灰石 + 榍石 + 锆石 + 钛铁矿。岩石未见明显矿化。蚀变不均, 以后期绿泥石化和碳酸盐化为主。

二长花岗斑岩 灰白色, 斑状结构, 块状构造(图 2C), 斑晶含量约为 20% ~ 40%, 矿物组合为石英(45%) + 斜长石(25%) + 钾长石(20%) + 角闪

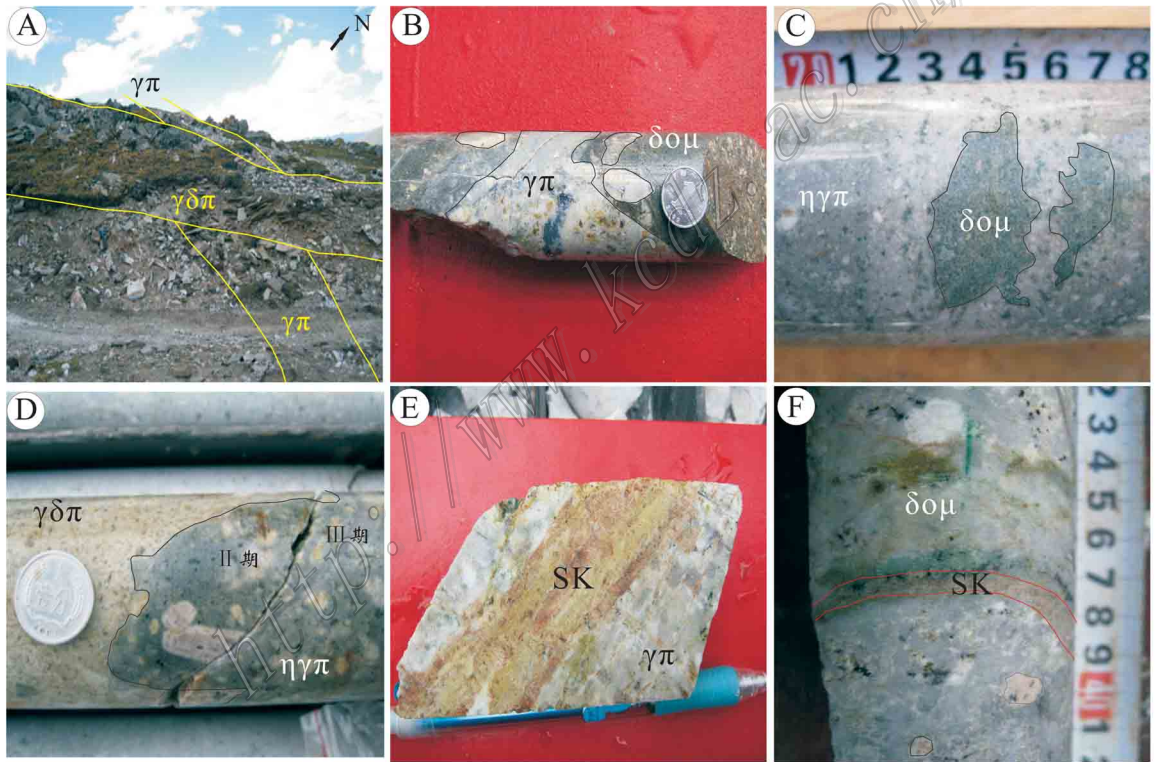


图 2 甲玛区内中酸性侵入岩的特征(1)

A. 花岗闪长斑岩脉切穿花岗斑岩(象背山地区); B. 石英闪长玢岩中的花岗斑岩捕虏体(ZK3216-286.5); C. 二长花岗斑岩中的石英闪长玢岩捕虏体(ZK4802-89); D. 二长花岗斑岩与花岗闪长斑岩接触带内的两期石英-辉钼矿脉(ZK1620-485); E. 矽卡岩脉切穿花岗斑岩(ZK815-582); F. 矽卡岩化石英闪长玢岩(ZK2007-104); $\gamma\pi$ —花岗斑岩; $\gamma\delta\pi$ —花岗闪长斑岩; $\delta\omicron\mu$ —石英闪长玢岩; $\eta\gamma\pi$ —二长花岗斑岩; SK—矽卡岩

Fig. 2 Characteristics of intermediate-acid intrusive rocks in the Jiama ore deposit (1)

A. Granitic porphyry cut by granodioritic porphyry (Xiangbeishan district); B. Granitic porphyry xenolith in quartz-dioritic porphyrite (ZK3216-286.5); C. Quartz-dioritic porphyrite xenolith in monzogranitic porphyry (ZK4802-89); D. Two stage quartz-molybdenite vein in the contact zone between monzogranitic porphyry and granodioritic porphyry (ZK1620-485); E. Granitic porphyry cut by skarn vein (ZK815-582); F. Skarnization quartz-dioritic porphyrite (ZK2007-104); $\gamma\pi$ —Granitic porphyry; $\gamma\delta\pi$ —Granodioritic porphyry; $\delta\omicron\mu$ —Quartz-dioritic porphyrite; $\eta\gamma\pi$ —Monzogranitic porphyry; SK—Skarn

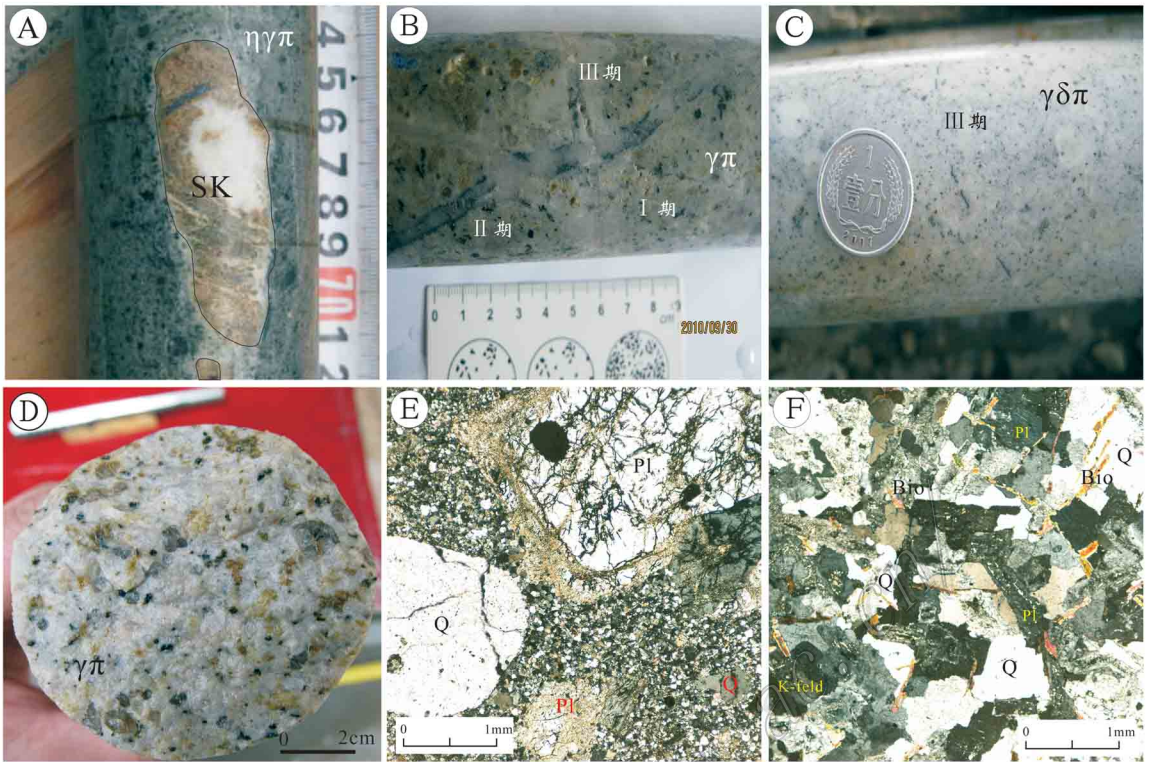


图3 甲玛矿区内中酸性侵入岩的特征(2)

A. 二长花岗斑岩中的砂卡岩捕虏体(ZK2412-130.1); B. 花岗斑岩中的三期石英-辉钼矿脉(ZK813-617); C. 花岗闪长斑岩中的辉钼矿脉(ZK813-617); D. 花岗斑岩(ZK001-象背山); E. 花岗斑岩(ZK001-象背山)的矿物组合, $d=4\text{ mm}$, 正交偏光; F. 二长花岗斑岩(ZK2412-130.1)的矿物组合, $d=4\text{ mm}$, 正交偏光; $\gamma\pi$ —花岗斑岩; $\gamma\delta\pi$ —花岗闪长斑岩; $\eta\gamma\pi$ —二长花岗斑岩; SK—砂卡岩; Q—石英; Pl—斜长石; Bio—黑云母; K-feld—钾长石

Fig. 3 Characteristics of intermediate-acid intrusive rocks in the Jiama deposit (2)

A. Skarn xenolith in monzogranitic porphyry (ZK2412-130.1); B. Three stage quartz-molybdenite vein in granitic porphyry (ZK813-617); C. Molybdenite vein in granodioritic porphyry (ZK813-617); D. Granitic porphyry (ZK001-Xiangbeishan district); E. Mineral association of granitic porphyry, $d=4\text{ mm}$, crossed nicols (ZK001-Xiangbeishan district); F. Mineral association of monzogranitic porphyry, $d=4\text{ mm}$, crossed nicols (ZK001-Xiangbeishan district); $\gamma\pi$ —Granitic porphyry; $\gamma\delta\pi$ —Granodioritic porphyry; $\eta\gamma\pi$ —Monzogranitic porphyry; SK—Skarn; Q—Quartz; Pl—Plagioclase; Bio—Biotite; K-feld—K-feldspar

石(10%)(图3F),副矿物组成为磷灰石+榍石+锆石+磁铁矿。岩石矿化不均,以Cu、Mo矿化为主,多呈细脉状构造。岩石中岩浆混合现象发育,以不规则产生的暗色铁镁质微粒包体(MME)、石英-黄铁矿(角闪石)眼斑(图3A)和斜长石发育不规则环带和海绵多孔状结构为标志。

3 分析测试方法

将岩石样品机械破碎,采用浮选和电磁选方法分选,在双目镜下挑选出锆石。然后,将这些锆石粘贴在环氧树脂表面,抛光后对锆石进行透射光、反射光及阴极发光显微照相。锆石的U-Pb同位素测试

在中国地质大学(北京)同位素室的LA-ICP-MS仪器(美国Agilent科技有限公司生产的7500a型)上完成,采用美国New Wave 193 SS激光器(分析点束斑直径为 $36\text{ }\mu\text{m}$)。年龄计算时,以标准锆石91500为外标进行同位素比值校正,TEM为监控标准样,元素含量以国际标样NIST612为外标、Si为内标进行计算。测试结果详见表1。

4 分析结果

4.1 锆石阴极发光特征

锆石CL图像如图4所示。该图中标出了多数测点的序号及其 $^{206}\text{Pb}/^{238}\text{U}$ 表面年龄值,有少量测点

表 1 甲玛矿床东凤垭(DFY)二长花岗斑岩和独立峰(DLF)、象背山(XBS)、塔龙尾(TLW)花岗岩锆石 LA-ICP-MS U-Pb 年龄数据

Table 1 LA-ICP-MS U-Pb data of zircons from Dongfengya (DFY) monzogranite porphyry and Duliufeng (DLF), Xiangbeishan (XBS), Talongwei (TLW) granite porphyry in the Jiama ore deposit

测点编号	$\epsilon_{\text{Zr}}(\text{B})/10^{-6}$						放射性同位素比值(误差 1σ)						年龄(误差 1σ)/Ma	
	Pb	Th	U	$^{207}\text{Pb}/^{206}\text{Pb}$	$^{207}\text{Pb}/^{235}\text{U}$	$^{206}\text{Pb}/^{238}\text{U}$	$^{238}\text{U}/^{232}\text{Th}$	$^{207}\text{Pb}/^{206}\text{Pb}$	$^{207}\text{Pb}/^{235}\text{U}$	$^{206}\text{Pb}/^{238}\text{U}$	$^{207}\text{Pb}/^{235}\text{U}$	$^{206}\text{Pb}/^{238}\text{U}$		
DFY-01	2.06	254.6	819.97	0.05425 ± 0.0074	0.01645 ± 0.00219	0.0022 ± 0.00007	3.22 ± 0.03	381 ± 240	17 ± 2	14.2 ± 0.5				
DFY-02	3.86	963.33	1360.23	0.03938 ± 0.00345	0.01245 ± 0.00108	0.00229 ± 0.00004	1.41 ± 0.01	-326 ± 169	13 ± 1	14.7 ± 0.5				
DFY-03	2.39	575.82	852.99	0.04992 ± 0.00457	0.01578 ± 0.00142	0.00229 ± 0.00005	1.48 ± 0.01	191 ± 162	16 ± 1	14.7 ± 0.5				
DFY-04	1.76	236.37	739.38	0.05996 ± 0.00933	0.01668 ± 0.00257	0.00205 ± 0.00007	3.13 ± 0.03	569 ± 281	17 ± 3	13.2 ± 0.5				
DFY-05	5.26	1327.46	1761.28	0.04336 ± 0.00307	0.01424 ± 0.00099	0.00238 ± 0.00004	1.33 ± 0.01	-104 ± 121	14.4 ± 1	15.3 ± 0.5				
DFY-06	3.25	612.36	1199.39	0.04324 ± 0.00361	0.01378 ± 0.00113	0.00231 ± 0.00004	1.96 ± 0.02	-110 ± 145	14 ± 1	14.9 ± 0.5				
DFY-07	1.05	385.76	322.54	0.05407 ± 0.01089	0.01729 ± 0.00343	0.00232 ± 0.00008	0.84 ± 0.01	374 ± 352	17 ± 3	14.9 ± 0.5				
DFY-08	3.39	1001.27	1112.62	0.04357 ± 0.00365	0.0141 ± 0.00116	0.00235 ± 0.00004	1.11 ± 0.01	-93 ± 147	14 ± 1	15.1 ± 0.3				
DFY-09	1.93	605.9	663.36	0.04774 ± 0.006	0.01501 ± 0.00185	0.00228 ± 0.00006	1.09 ± 0.01	86 ± 220	15 ± 2	14.7 ± 0.4				
DFY-10	2.82	72.12	97.77	0.04851 ± 0.00438	0.015479 ± 0.01371	0.02314 ± 0.00047	1.36 ± 0.01	124 ± 159	146 ± 12	147 ± 3				
DFY-11	3.77	1064.1	1271.89	0.04941 ± 0.00291	0.01566 ± 0.0009	0.0023 ± 0.00004	1.2 ± 0.01	167 ± 99	15.8 ± 0.9	14.8 ± 0.3				
DFY-12	3.77	742.89	1369.98	0.04823 ± 0.00285	0.01554 ± 0.0009	0.00234 ± 0.00004	1.84 ± 0.02	111 ± 98	15.7 ± 0.9	15.1 ± 0.3				
DFY-13	4.39	1370.09	1513.61	0.046 ± 0.00282	0.01426 ± 0.00086	0.00225 ± 0.00003	1.1 ± 0.01	-2 ± 105	14.4 ± 0.9	14.5 ± 0.2				
DFY-14	3.33	609.43	1184.98	0.05237 ± 0.00365	0.0168 ± 0.00115	0.00233 ± 0.00004	1.94 ± 0.02	302 ± 125	17 ± 1	15 ± 0.3				
DFY-15	1.95	340.83	717.97	0.04151 ± 0.00432	0.01347 ± 0.00138	0.00235 ± 0.00004	2.11 ± 0.02	-204 ± 161	14 ± 1	15.1 ± 0.3				
DFY-16	4.25	936.31	1560.49	0.04634 ± 0.00264	0.01445 ± 0.00081	0.00226 ± 0.00003	1.67 ± 0.02	15 ± 95	14.6 ± 0.8	14.6 ± 0.2				
DFY-17	4.15	1032.91	1417.13	0.0465 ± 0.00267	0.0152 ± 0.00086	0.00257 ± 0.00004	1.37 ± 0.01	24 ± 90	15.3 ± 0.9	15.3 ± 0.3				
DFY-18	2.96	663.42	1075.99	0.04561 ± 0.00346	0.01435 ± 0.00107	0.00228 ± 0.00004	1.62 ± 0.02	-23 ± 129	14 ± 1	14.7 ± 0.3				
DFY-19	3.05	761.13	1076.62	0.0448 ± 0.00338	0.01439 ± 0.00107	0.00233 ± 0.00004	1.41 ± 0.01	-30 ± 129	15 ± 1	15 ± 0.3				
DFY-20	2.97	626.01	1052.83	0.05003 ± 0.00325	0.01596 ± 0.00102	0.00231 ± 0.00004	1.68 ± 0.02	196 ± 114	16 ± 1	14.9 ± 0.3				
DFY-21	3.45	680.09	1330.4	0.04472 ± 0.00307	0.01358 ± 0.00092	0.0022 ± 0.00003	1.96 ± 0.02	-34 ± 121	13.7 ± 0.9	14.2 ± 0.2				
DFY-22	2.36	777.96	781.22	0.04649 ± 0.00382	0.01476 ± 0.00119	0.0023 ± 0.00004	1 ± 0.01	23 ± 144	15 ± 1	14.8 ± 0.3				
DFY-23	3.97	2483.83	1023.6	0.04962 ± 0.00601	0.01502 ± 0.00178	0.00219 ± 0.00006	0.41 ± 0.01	177 ± 215	15 ± 2	14.1 ± 0.4				
DFY-24	3.75	884.58	1319.67	0.04615 ± 0.00298	0.0148 ± 0.00094	0.00233 ± 0.00004	1.49 ± 0.01	5 ± 105	14.9 ± 0.9	15 ± 0.3				
DFY-25	3.31	660.72	1185.57	0.04859 ± 0.0032	0.01571 ± 0.00101	0.00234 ± 0.00004	1.79 ± 0.02	128 ± 112	16 ± 1	15.1 ± 0.3				
DLF-01	2.81	547.76	1060.86	0.04686 ± 0.00444	0.01427 ± 0.00133	0.00221 ± 0.00005	1.94 ± 0.02	42 ± 163	14 ± 1	14.2 ± 0.3				
DLF-02	4.16	779.17	1494.4	0.04219 ± 0.00277	0.01362 ± 0.00088	0.00234 ± 0.00004	1.92 ± 0.02	-167 ± 112	13.7 ± 0.9	15.1 ± 0.3				
DLF-03	0.80	248	265.16	0.05254 ± 0.00846	0.01659 ± 0.00263	0.00229 ± 0.00007	1.07 ± 0.01	309 ± 295	17 ± 3	14.7 ± 0.5				
DLF-04	0.82	241.65	248.2	0.04221 ± 0.01029	0.01454 ± 0.00352	0.0025 ± 0.00008	1.03 ± 0.01	-166 ± 319	15 ± 4	16.1 ± 0.5				
DLF-05	3.21	663.12	1143.5	0.0446 ± 0.0032	0.01422 ± 0.001	0.00231 ± 0.00004	1.72 ± 0.02	-40 ± 120	14 ± 1	14.9 ± 0.3				
DLF-06	1.80	724.58	536.94	0.04857 ± 0.00483	0.01579 ± 0.00155	0.00236 ± 0.00005	0.74 ± 0.01	127 ± 180	16 ± 2	15.2 ± 0.3				
DLF-07	3.99	798.38	1466.67	0.04391 ± 0.00272	0.01387 ± 0.00084	0.00229 ± 0.00004	1.84 ± 0.02	-75 ± 98	14 ± 0.8	14.7 ± 0.3				

续表 1-1
Cont. Table 1-1

测点编号	$w(B)/10^{-6}$			放射性同位素比值(误差 1σ)					年龄(误差 1σ)/Ma		
	Pb	Th	U	$^{207}\text{Pb}/^{235}\text{U}$	$^{206}\text{Pb}/^{238}\text{U}$	$^{238}\text{U}/^{232}\text{Th}$	$^{207}\text{Pb}/^{206}\text{Pb}$	$^{207}\text{Pb}/^{235}\text{U}$	$^{206}\text{Pb}/^{238}\text{U}$		
DLF-08	5.29	860.23	2039.39	0.04419 ± 0.00241	0.00225 ± 0.00003	2.37 ± 0.02	-61 ± 89	13.8 ± 0.7	14.5 ± 0.2		
DLF-09	1.61	607.6	506.92	0.04511 ± 0.00583	0.00227 ± 0.00005	0.83 ± 0.01	-14 ± 211	14 ± 2	14.6 ± 0.3		
DLF-10	1.30	358.5	424.84	0.04833 ± 0.00695	0.00238 ± 0.00006	1.19 ± 0.01	115 ± 251	16 ± 2	15.3 ± 0.4		
DLF-11	0.99	326.34	303.7	0.04452 ± 0.00781	0.00245 ± 0.00007	0.93 ± 0.01	-44 ± 251	15 ± 3	15.8 ± 0.5		
DLF-12	2.33	637.96	777.97	0.04789 ± 0.00502	0.00232 ± 0.00005	1.22 ± 0.01	94 ± 189	15 ± 2	14.9 ± 0.3		
DLF-13	2.37	542.02	791.41	0.05076 ± 0.00491	0.00243 ± 0.00005	1.46 ± 0.01	230 ± 177	17 ± 2	15.6 ± 0.3		
DLF-14	3.53	755.1	1176.11	0.05071 ± 0.00346	0.00244 ± 0.00004	1.56 ± 0.02	228 ± 123	17 ± 1	15.7 ± 0.3		
DLF-15	2.88	572.67	936.97	0.04366 ± 0.00354	0.00257 ± 0.00004	1.64 ± 0.02	-88 ± 145	16 ± 1	16.5 ± 0.3		
DLF-16	1.08	425.95	320.53	0.04379 ± 0.00936	0.0024 ± 0.00007	0.75 ± 0.01	-81 ± 288	15 ± 3	15.5 ± 0.5		
DLF-17	1.77	307.65	652.8	0.04377 ± 0.00553	0.00234 ± 0.00006	2.12 ± 0.02	-82 ± 186	14 ± 2	15.1 ± 0.4		
DLF-18	2.60	784.15	638.83	0.04923 ± 0.00667	0.0024 ± 0.00005	0.81 ± 0.01	159 ± 276	16 ± 2	15.5 ± 0.3		
DLF-19	1.73	622.13	522.77	0.04631 ± 0.00553	0.0024 ± 0.00005	0.84 ± 0.01	14 ± 209	15 ± 2	15.5 ± 0.3		
DLF-20	1.25	436.25	370.84	0.04769 ± 0.00776	0.00242 ± 0.00006	0.85 ± 0.01	84 ± 274	16 ± 3	15.6 ± 0.4		
DLF-21	1.39	525.33	401.79	0.04445 ± 0.00602	0.00247 ± 0.00006	0.76 ± 0.01	-47 ± 205	15 ± 2	15.9 ± 0.4		
DLF-22	1.60	345.37	527.07	0.04757 ± 0.0052	0.00254 ± 0.00005	1.53 ± 0.02	78 ± 200	17 ± 2	16.4 ± 0.3		
DLF-23	2.31	483.78	813.87	0.04926 ± 0.00501	0.00237 ± 0.00005	1.68 ± 0.02	160 ± 185	16 ± 2	15.3 ± 0.3		
DLF-24	4.26	880.71	1579.97	0.04702 ± 0.00274	0.00229 ± 0.00004	1.79 ± 0.02	50 ± 92	15 ± 0.9	14.7 ± 0.3		
DLF-25	2.63	378.57	950.41	0.0505 ± 0.00416	0.00241 ± 0.00005	2.51 ± 0.03	218 ± 145	17 ± 1	15.5 ± 0.3		
TLW-01	0.83	203.28	252.98	0.04384 ± 0.01023	0.00262 ± 0.00008	1.24 ± 0.01	-79 ± 317	16 ± 4	16.9 ± 0.5		
TLW-02	0.98	223.45	325.62	0.04846 ± 0.00781	0.0025 ± 0.00007	1.46 ± 0.01	122 ± 270	17 ± 3	16.1 ± 0.5		
TLW-03	1.43	433.54	422.68	0.04836 ± 0.00634	0.00251 ± 0.00006	0.97 ± 0.01	117 ± 237	17 ± 2	16.2 ± 0.4		
TLW-04	1.42	538.86	413.99	0.04075 ± 0.00645	0.00253 ± 0.00007	0.77 ± 0.01	-247 ± 213	14 ± 2	16.3 ± 0.5		
TLW-05	2.18	595.12	676.21	0.04626 ± 0.0046	0.00255 ± 0.00005	1.14 ± 0.01	11 ± 179	16 ± 2	16.4 ± 0.3		
TLW-06	0.30	128.56	92.41	0.02891 ± 0.03129	0.00224 ± 0.00015	0.72 ± 0.01	-332 ± 965	9 ± 10	14.4 ± 1		
TLW-07	1.27	487.2	353.31	0.04351 ± 0.00754	0.00256 ± 0.00007	0.73 ± 0.01	-96 ± 241	15 ± 3	16.5 ± 0.5		
TLW-08	1.89	762.58	578.71	0.05016 ± 0.00874	0.00223 ± 0.00008	0.76 ± 0.01	202 ± 289	16 ± 3	14.4 ± 0.5		
TLW-09	1.31	293.21	390.39	0.04741 ± 0.00682	0.00261 ± 0.00006	1.33 ± 0.01	70 ± 247	17 ± 2	16.8 ± 0.4		
TLW-10	1.66	261.46	523.67	0.04837 ± 0.00715	0.00265 ± 0.00008	2 ± 0.02	117 ± 251	18 ± 3	17.1 ± 0.5		
TLW-11	1.13	330.35	318.54	0.04726 ± 0.00785	0.00264 ± 0.00007	0.96 ± 0.01	62 ± 267	17 ± 3	17 ± 0.5		
TLW-12	1.30	574.91	371.4	0.03484 ± 0.00885	0.00229 ± 0.00007	0.65 ± 0.01	-80 ± 298	11 ± 3	14.7 ± 0.5		
TLW-13	0.72	156.62	265.14	0.03945 ± 0.01242	0.00232 ± 0.0001	1.69 ± 0.02	-322 ± 406	13 ± 4	14.9 ± 0.6		
TLW-14	1.71	958.13	429.65	0.05 ± 0.01048	0.00226 ± 0.0001	0.45 ± 0.01	195 ± 325	16 ± 3	14.6 ± 0.6		
TLW-15	1.05	298.61	339.96	0.04833 ± 0.01139	0.00236 ± 0.00011	1.14 ± 0.01	15 ± 341	16 ± 4	15.2 ± 0.7		

续表 1-2
Cont. Table 1-2

测点编号	$\omega(B)/10^{-6}$				放射性同位素比值(误差 1 σ)				年龄(误差 1 σ)/Ma			
	Pb	Th	U		$^{207}\text{Pb}/^{206}\text{Pb}$	$^{207}\text{Pb}/^{235}\text{U}$	$^{206}\text{Pb}/^{238}\text{U}$	$^{238}\text{U}/^{232}\text{Th}$	$^{207}\text{Pb}/^{206}\text{Pb}$	$^{207}\text{Pb}/^{235}\text{U}$	$^{206}\text{Pb}/^{238}\text{U}$	$^{206}\text{Pb}/^{238}\text{U}$
TLW-16	3.42	564.46	1224.51		0.0508 ± 0.00434	0.01676 ± 0.0014	0.00239 ± 0.00005	2.17 ± 0.02	232 ± 151	17 ± 1	15.4 ± 0.3	15.4 ± 0.3
TLW-17	1.77	380.58	571.93		0.04872 ± 0.00617	0.01626 ± 0.00202	0.00242 ± 0.00006	1.5 ± 0.02	134 ± 229	16 ± 2	15.6 ± 0.4	15.6 ± 0.4
TLW-18	2.15	868.94	581.52		0.04598 ± 0.00483	0.01589 ± 0.00165	0.00251 ± 0.00005	0.67 ± 0.01	-3 ± 190	16 ± 2	16.2 ± 0.3	16.2 ± 0.3
TLW-19	0.56	217.56	173.05		0.04767 ± 0.01495	0.01533 ± 0.00474	0.00233 ± 0.00012	0.8 ± 0.01	83 ± 441	15 ± 5	15 ± 0.8	15 ± 0.8
TLW-20	1.08	326.48	315.96		0.04362 ± 0.00754	0.01584 ± 0.00271	0.00263 ± 0.00007	0.97 ± 0.01	-90 ± 241	16 ± 3	16.9 ± 0.5	16.9 ± 0.5
TLW-21	0.75	221.24	219.12		0.04447 ± 0.01115	0.01627 ± 0.00403	0.00265 ± 0.00011	0.99 ± 0.01	-46 ± 331	16 ± 4	17.1 ± 0.7	17.1 ± 0.7
TLW-22	0.91	265.8	286.54		0.05026 ± 0.01089	0.01754 ± 0.00376	0.00253 ± 0.00008	1.08 ± 0.01	207 ± 349	18 ± 4	16.3 ± 0.5	16.3 ± 0.5
TLW-23	1.07	361.54	315.9		0.04607 ± 0.01436	0.01398 ± 0.00431	0.0022 ± 0.0001	0.87 ± 0.01	1 ± 502	14 ± 4	14.2 ± 0.6	14.2 ± 0.6
TLW-24	0.53	143.97	180.36		0.06511 ± 0.01961	0.02014 ± 0.00596	0.00224 ± 0.00013	1.25 ± 0.01	778 ± 512	20 ± 6	14.4 ± 0.8	14.4 ± 0.8
TLW-25	1.37	385.68	427.29		0.04405 ± 0.00704	0.01476 ± 0.00233	0.00243 ± 0.00007	1.11 ± 0.01	-68 ± 225	15 ± 2	15.6 ± 0.5	15.6 ± 0.5
XBS-01	0.85	285.93	255.44		0.04745 ± 0.0101	0.016 ± 0.00338	0.00244 ± 0.00007	0.89 ± 0.01	72 ± 329	16 ± 3	15.7 ± 0.5	15.7 ± 0.5
XBS-02	1.45	582.83	410.41		0.04343 ± 0.00758	0.01462 ± 0.00253	0.00244 ± 0.00006	0.7 ± 0.01	-100 ± 247	15 ± 3	15.9 ± 0.4	15.9 ± 0.4
XBS-03	1.47	449.3	446.85		0.04379 ± 0.00668	0.01489 ± 0.00225	0.00247 ± 0.00006	0.99 ± 0.01	-81 ± 221	15 ± 2	15.9 ± 0.4	15.9 ± 0.4
XBS-04	0.70	84.18	234.52		0.04765 ± 0.01722	0.0135 ± 0.00483	0.00205 ± 0.00011	0.83 ± 0.01	82 ± 515	14 ± 5	13.2 ± 0.7	13.2 ± 0.7
XBS-05	1.01	276.94	260.19		0.04605 ± 0.00389	0.01645 ± 0.00134	0.00259 ± 0.00006	0.94 ± 0.01	± 186	17 ± 1	16.7 ± 0.4	16.7 ± 0.4
XBS-06	1.53	746.32	356.98		0.05064 ± 0.00773	0.01802 ± 0.00272	0.00258 ± 0.00006	0.48 ± 0.01	224 ± 278	18 ± 3	16.6 ± 0.4	16.6 ± 0.4
XBS-07	0.56	106.33	164.23		0.04652 ± 0.02025	0.01842 ± 0.00793	0.00287 ± 0.00019	1.54 ± 0.02	25 ± 609	19 ± 8	18 ± 1	18 ± 1
XBS-08	0.92	331.86	265.48		0.04364 ± 0.01052	0.01504 ± 0.0036	0.0025 ± 0.00007	0.8 ± 0.01	-89 ± 330	15 ± 4	16.1 ± 0.5	16.1 ± 0.5
XBS-09	0.99	290	301.67		0.051 ± 0.01038	0.01759 ± 0.00352	0.0025 ± 0.0001	1.04 ± 0.01	241 ± 334	18 ± 4	16.1 ± 0.6	16.1 ± 0.6
XBS-10	1.20	480.43	348.16		0.04294 ± 0.00799	0.0141 ± 0.00259	0.00238 ± 0.00007	0.72 ± 0.01	-126 ± 247	14 ± 3	15.3 ± 0.5	15.3 ± 0.5
XBS-11	0.95	436.51	253.82		0.04284 ± 0.00936	0.01394 ± 0.00302	0.00236 ± 0.00007	0.58 ± 0.01	-132 ± 291	14 ± 3	15.2 ± 0.5	15.2 ± 0.5
XBS-12	1.29	489.44	377.76		0.04497 ± 0.008	0.01509 ± 0.00266	0.00243 ± 0.00006	0.77 ± 0.01	-21 ± 262	15 ± 3	15.6 ± 0.4	15.6 ± 0.4
XBS-13	1.26	470.53	341.78		0.08366 ± 0.00906	0.02873 ± 0.00301	0.00249 ± 0.00007	0.73 ± 0.01	1285 ± 162	29 ± 3	16 ± 0.5	16 ± 0.5
XBS-14	1.90	468.77	589.94		0.04802 ± 0.00499	0.01723 ± 0.00177	0.0026 ± 0.00005	1.26 ± 0.01	100 ± 193	17 ± 2	16.7 ± 0.3	16.7 ± 0.3
XBS-15	1.36	382.77	426.85		0.04339 ± 0.00624	0.01504 ± 0.00214	0.00251 ± 0.00006	1.12 ± 0.01	-102 ± 206	15 ± 2	16.2 ± 0.4	16.2 ± 0.4
XBS-16	0.69	206.67	191		0.04849 ± 0.012	0.01794 ± 0.00438	0.00268 ± 0.00012	0.92 ± 0.01	123 ± 366	18 ± 4	17.3 ± 0.8	17.3 ± 0.8
XBS-17	1.47	668.8	343.27		0.04908 ± 0.00982	0.01796 ± 0.00355	0.00265 ± 0.00009	0.51 ± 0.01	152 ± 316	18 ± 4	17.1 ± 0.6	17.1 ± 0.6
XBS-18	0.59	162.28	174.29		0.04438 ± 0.01304	0.01633 ± 0.00476	0.00267 ± 0.0001	1.07 ± 0.01	-51 ± 398	16 ± 5	17.2 ± 0.6	17.2 ± 0.6
XBS-19	0.57	216.51	167.62		0.04661 ± 0.01382	0.01503 ± 0.00442	0.00234 ± 0.00009	0.77 ± 0.01	29 ± 427	15 ± 4	15.1 ± 0.6	15.1 ± 0.6
XBS-20	1.41	303.93	465.21		0.04548 ± 0.00866	0.01528 ± 0.00286	0.00244 ± 0.00009	1.55 ± 0.02	-30 ± 273	15 ± 3	15.7 ± 0.6	15.7 ± 0.6
XBS-21	0.79	284.41	240.38		0.04271 ± 0.01057	0.01429 ± 0.00351	0.00243 ± 0.00008	0.85 ± 0.01	-139 ± 325	14 ± 4	15.6 ± 0.5	15.6 ± 0.5
XBS-22	0.88	295.6	261.92		0.04546 ± 0.00897	0.01582 ± 0.00309	0.00252 ± 0.00007	0.89 ± 0.01	-31 ± 294	16 ± 3	16.2 ± 0.5	16.2 ± 0.5
XBS-23	1.39	605.62	380.23		0.04435 ± 0.00812	0.01509 ± 0.00274	0.00247 ± 0.00006	0.63 ± 0.01	-53 ± 264	15 ± 3	15.9 ± 0.4	15.9 ± 0.4
XBS-24	0.55	214.01	155.37		0.06556 ± 0.01312	0.02269 ± 0.00447	0.00251 ± 0.0001	0.73 ± 0.01	792 ± 363	23 ± 4	16.2 ± 0.6	16.2 ± 0.6
XBS-25	0.93	311.16	279.17		0.04614 ± 0.00947	0.01562 ± 0.00318	0.00246 ± 0.00007	0.9 ± 0.01	5 ± 31	16 ± 3	15.8 ± 0.5	15.8 ± 0.5

测试单位: 中国地质大学(北京)地质实验室测试中心。

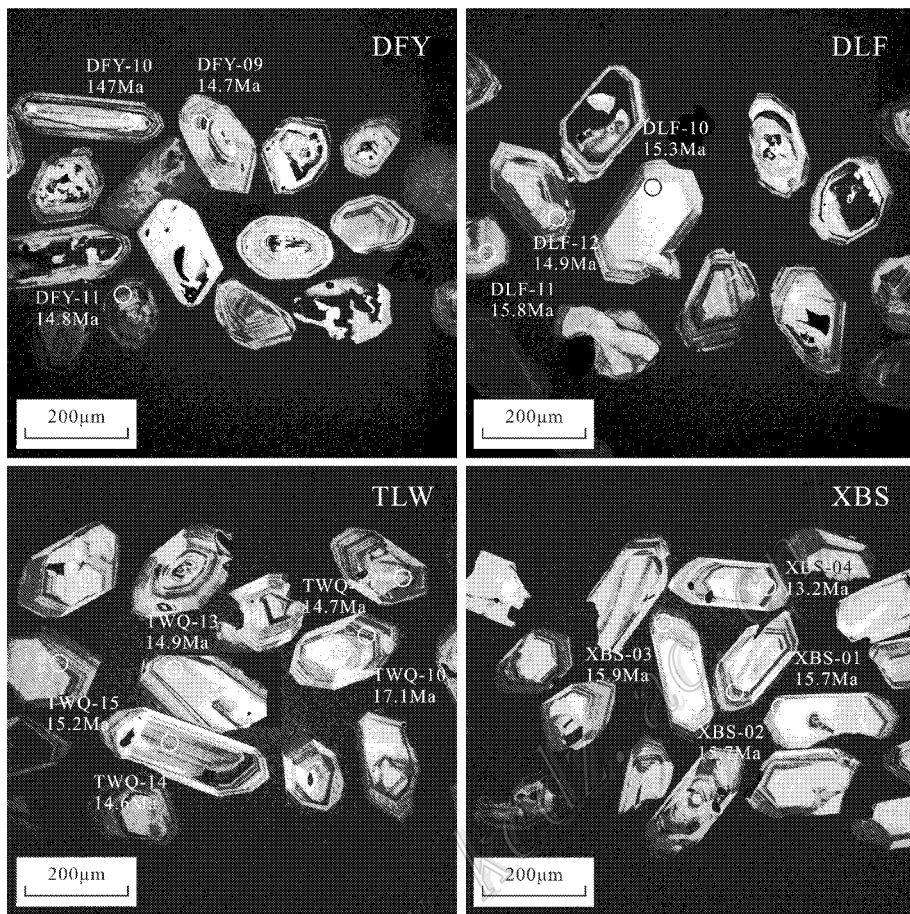


图4 甲玛矿床内酸性侵入岩中锆石的阴极发光图像

Fig. 4 Cathodoluminescence images of zircons in intermediate-acid intrusive rocks from the Jiama deposit

因未在所示的 CL 图像中,故而未予标出。

根据 CL 形态特征可见,所分选出来的锆石均为无色透明,呈长柱状自形晶体,有少量发生了碎裂,其长轴长度为 $100 \sim 250 \mu\text{m}$,长短轴之比为 $2:1 \sim 3:1$,具有明显的震荡环带,均为同源岩浆锆石(Hanchar et al., 1993)。4 件样品的 Th/U 比值多数大于 0.4(仅 DFY-01 测点为 0.4 以及 DLF-25 测点小于 0.4),具有一般岩浆成因锆石的特征,并受到热液混染和改造。锆石受外来熔体/流体的混染和改造有 2 种表现形式:① 岛湾状构造(Liati et al., 1999; Rubatto et al., 1999, 2003; Zheng et al., 2007);② 不规则白色环边或团斑,显示出原生锆石已发生重结晶作用(Corfu et al., 2003)。

4.2 锆石 U-Pb 年龄

对 4 件岩体样品内锆石所测得的 $^{206}\text{Pb}/^{238}\text{U}$ 表面年龄值的变化范围较大(表 1),显示出原生锆石在岩浆混合及后期蚀变过程中,Pb 有部分丢失。排除丢失铅对加权平均年龄值的影响后,塔龙尾花岗斑

岩体(TLW)16 个测点的加权平均年龄值为 $(16.27 \pm 0.31) \text{Ma}$ (1σ , MSWD = 1.9);象背山花岗斑岩体(XBS)20 个测点的加权平均年龄值为 $(15.99 \pm 0.34) \text{Ma}$ (1σ , MSWD = 2.5);独立峰花岗斑岩体(DLF)24 个测点的加权平均年龄值为 $(15.31 \pm 0.24) \text{Ma}$ (1σ , MSWD = 3.8);东风垭二长花岗斑岩脉(DFY)19 个测点的加权平均年龄值为 $(14.81 \pm 0.16) \text{Ma}$ (1σ , MSWD = 1.5)(图 5)。测点年龄的计算均用 Isoplot 软件(Ludwig et al., 1999)处理,较为客观、真实地反映了这 4 个岩体的侵位时限。

由测试结果可见,花岗斑岩的侵位时间早于二长花岗斑岩。此外,在东风垭(DFY)二长花岗斑岩脉中发现了一颗捕虏锆石(长短比 $4:1$,具震荡环带),其年龄值为 147 Ma(DFY-10, Th/U 比值为 0.74),接近于冈底斯带内晚侏罗世橄榄玄粗岩的岩浆活动期(Aitchison et al., 2007),推测甲玛二长花岗斑岩体的形成可能源自晚侏罗世侵位的深部玄武质岩石的重熔。

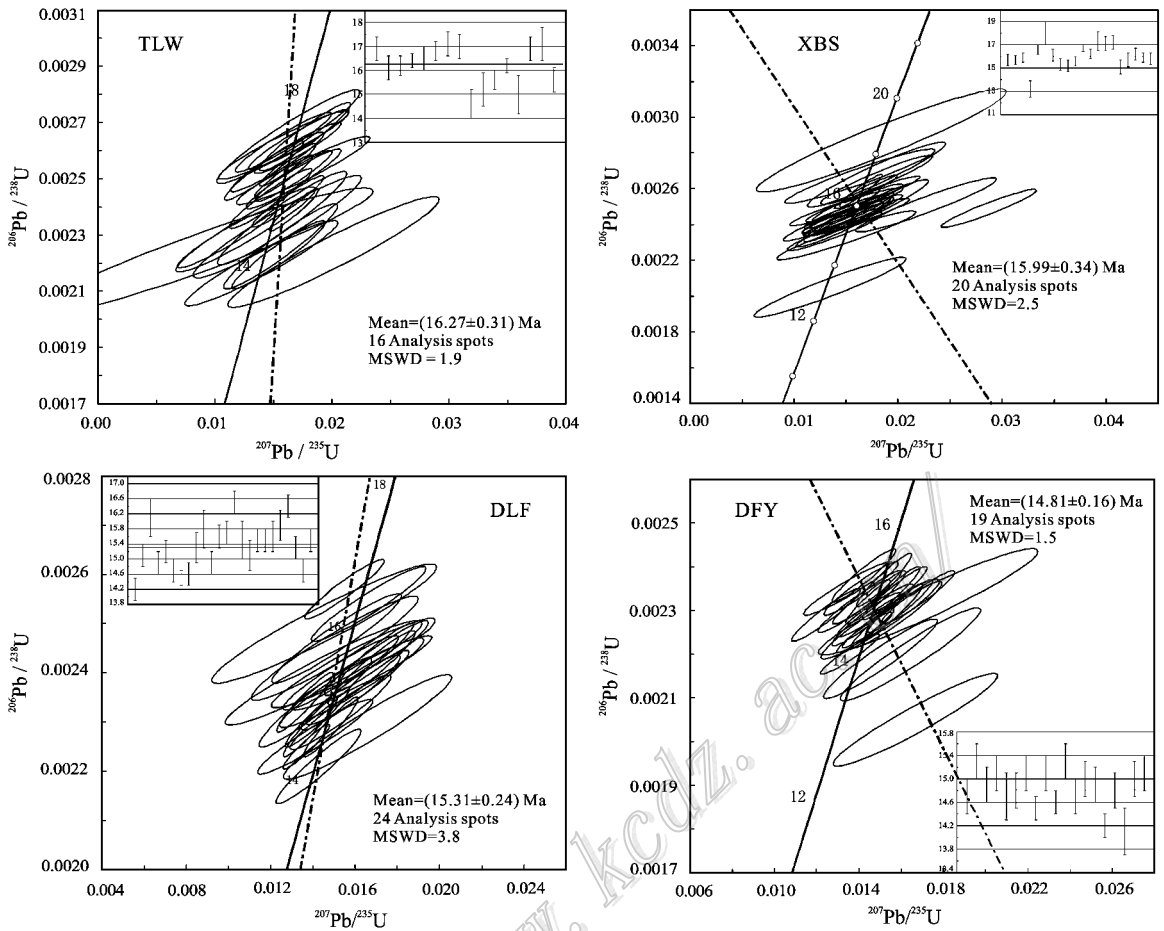


图5 甲玛矿区塔龙尾(TLW)、象背山(XBS)、独立峰(DLF)花岗斑岩及东风垭(DFY)二长花岗斑岩内锆石U-Pb年龄谐和图

Fig. 5 Concordia diagrams for U-Pb ages of zircon grains in Talongwei (TLW), Xiangbeishan (XBS), Dulifeng (DLF) granite porphyry and Dongfengya (DFY) monzogranite porphyry from the Jiama ore deposit

5 讨论

5.1 岩体(脉)侵位时序的厘定

测年结果(表1及图5)总体显示出,花岗斑岩早于二长花岗斑岩,并且花岗斑岩的侵位以塔龙尾为中心,沿东西向向两侧演化,侵位于褶皱的转折端。可以推测,在该矿区红-塔背斜至牛马塘背斜之间,应该存在隐伏的花岗斑岩体,甲玛隐伏斑岩体(花岗斑岩)的发现,已证实了这一推断。

此外,花岗闪长斑岩(图2A)和石英闪长玢岩(图2B)存在不同程度的切穿,以及捕虏花岗斑岩,暗示了两者的侵位晚于花岗斑岩。在该矿区范围内,二长花岗斑岩、花岗闪长斑岩和石英闪长玢岩的相互关系较为明显,其中,石英闪长玢岩的侵位早于花岗闪长斑岩、二长花岗斑岩,后两者内常包含有石

英闪长玢岩的不规则包体(图2C)。花岗闪长斑岩则侵位最晚,在接触面上可见花岗闪长斑岩的冷凝边构造及二长花岗斑岩的港湾状构造(图2D)。

综上所述,甲玛矿区内中酸性斑岩的侵位时序为:花岗斑岩(15.31~16.27 Ma)—石英闪长玢岩—二长花岗斑岩(14.81 Ma)—花岗闪长斑岩。同位素测年结果证实了地质证据的正确性。

5.2 岩浆-成矿作用

甲玛矿床的形成与岩浆作用密不可分,岩浆活动的多期多阶段性导致了成矿作用的多期多阶段性,宏观上表现为石英-硫化物脉的多期产出。以石英-辉钼矿为例,随着岩浆作用的不断进行,成矿过程显示出3期不同程度的成矿作用(图3B),具体表现为:

I期成矿作用 目前发现,仅在花岗斑岩及石英闪长玢岩中发育(图3B),呈近直立的粗脉浸染状构造,矿物组合为石英+辉钼矿+(阳起石或黑云

母)矿石内辉钼矿的 Re-Os 同位素年龄为 15.3 Ma 左右(应立娟等 2009),为花岗斑岩或石英闪长玢岩岩浆活动之后的一次成矿作用。

Ⅱ期成矿作用 发育在花岗斑岩、石英闪长玢岩和二长花岗斑岩中,呈大角度(轴交角在 30°左右)切层产出,细脉浸染状构造,矿物组合为石英+辉钼矿+(石膏)。在图 2D 中明确指示了该期成矿作用与岩浆活动的关系:Ⅱ期石英+辉钼矿脉切穿二长花岗斑岩但被花岗闪长斑岩所截,是二长花岗斑岩之后花岗闪长斑岩之前的成矿作用,与二长花岗斑岩的岩浆活动相对应。

Ⅲ期成矿作用 在所有岩浆岩中均有不同程度的发育,呈小角度(轴交角在 60°左右)切层产出,细脉浸染状构造,矿物组合为石英+辉钼矿+(石膏),表现为花岗闪长斑岩之后的成矿作用过程,与花岗闪长斑岩的岩浆活动相对应。

此外,对所有岩浆岩的基本分析结果显示:矿化最好的为花岗斑岩(M_o 加权平均值为 0.04%),其次为二长花岗斑岩(M_o 加权平均值为 0.02%),最差的为花岗闪长斑岩(M_o 加权平均值 < 0.01%)。这从侧面反映了多期成矿作用对矿质富集的制约,表明甲玛矿床的形成是 3 期岩浆-成矿作用相互叠加的直接结果。

6 结论

(1)西藏甲玛矿区内中酸性斑岩发育,呈岩株或岩脉产出。受区域构造活动的影响,花岗斑岩位于褶皱转折端,石英闪长玢岩、二长花岗斑岩和花岗闪长斑岩近直立产出,呈近 NS 向雁列式展布。岩体侵位及矽卡岩形成的时序为:花岗斑岩(15.31~16.27 Ma)—石英闪长玢岩—二长花岗斑岩(14.81 Ma)—花岗闪长斑岩。

(2)甲玛矿床可分出 3 期成矿作用,每期成矿作用分别对应于花岗斑岩或石英闪长玢岩、二长花岗斑岩及花岗闪长斑岩 3 期不同强度的岩浆作用。甲玛矿床的形成是 3 期岩浆-成矿作用叠加的结果。

志 谢 在本文完成过程中,中国地质大学(北京)实验测试中心的苏黎老师给予了无私的帮助和指导,在此表示衷心感谢!

References

Aitchison J C, McDermid I R C, Ali J R, Davis A M and Zyabrev S V.

2007. Shoshonites in Southern Tibet record Late Jurassic rifting of a Tethyan intraoceanic island arc [J]. *Journal of Geology*, 115 : 197-213.
- Coleman M and Hodges K. 1995. Evidence for Tibetan plateau uplift before 14 Myr ago from a new minimum age for east-west extension [J]. *Nature*, 374 : 49-52.
- Corfu F, Hanchar J M, Hoskin P W O and Kinny P. 2003. Atlas of zircon textures [J]. *Mineralogy and Geochemistry*, 53 : 469-500.
- Hanchar J M, Miller C F. 1993. Zircon zonation patterns as revealed by cathodoluminescence and backscattered electron images: Implications for interpretation of complex crustal histories [J]. *Chemical Geology*, 110 : 1-13.
- Harrison T M, Copeland P and Kidd W S F. 1995. Activation of the Nyainqentanghla shear zone: Implication for uplift of the southern Tibetan Plateau [J]. *Tectonics*, 14 : 658-676.
- Liati A and Gebauer D. 1999. Constraining the prograde and retrograde P-T-t path of Eocene HP rocks by SHRIMP dating difference zircon domain: Inferred rates of heating-burial, cooling and exhumation for central Rhodope, northern Greece [J]. *Contributions to Mineralogy and Petrology*, 135 : 340-354.
- Ludwig A K R. 1999. Using Isoplot/EX, version 3.23, A geochronological toolkit for Microsoft Excel [CP]. Berkeley: Berkeley Geochronological Center Special Publication, 47.
- Rubatto D, Gebauer G and Compagnoni R. 1999. Dating of eclogite-facies zircons: The age of Alpine metamorphism in the Sesia-Lanzo Zone (Western Alps) [J]. *Earth and Planetary Science Letters*, 167 : 141-158.
- Rubatto D and Hermann J. 2003. Zircon formation during fluid circulation in eclogites (Monviso, Western Alps): Implications for Zr and Hf budget in subduction zones [J]. *Geochimica et Cosmochimica Acta*, 67 : 2173-2187.
- Tang J X, Wang D H, Wang X W, Zhong K H, Ying L J, Zheng W B, Li F J, Guo N, Qin Z P, Yao X F, Li L, Wang Y and Tang X Q. 2010. Geological features and metallogenic model of the Jiama copper-polymetallic deposit in Tibet [J]. *Acta Geoscientia Sinica*, 31 (4): 1-12 (in Chinese with English abstract).
- Yin A and Harrison T M. 2000. Geological evolution of the Himalayan-Tibetan orogen [J]. *Annu. Rev. Earth Planet. Sci. Lett.*, 28 : 21-280.
- Ying L J, Tang J X, Wang D H, Chang Z S, Qu W J and Zheng W B. 2009. Re-Os isotopic dating of molybdenite in skarn from the Jiama copper-polymetallic deposit of Tibet and its metallogenic significance [J]. *Rock and Mineral Analysis*, 3 : 265-268 (in Chinese with English abstract).
- Zheng Y F, Gao T S, Wu Y B, Gong B and Liu X M. 2007. Fluid flow during exhumation of deeply subducted continental crust: Zircon U-Pb age and O-isotope studies of a quartz vein within ultrahigh-pressure eclogite [J]. *Journal of Metamorphic Geology*, 25 : 267-283.

附中文参考文献

- 唐菊兴,王登红,汪雄武,钟康惠,应立娟,郑文宝,黎枫信,郭娜,秦志鹏,姚晓峰,李磊,王友,唐晓倩. 2010. 西藏甲玛铜多金属矿床地质特征及其矿床模型 [J]. *地球学报*, 31(4): 1-12.
- 应立娟,唐菊兴,王登红,畅哲生,屈文俊,郑文宝. 2009. 西藏甲玛铜多金属矿床矽卡岩中辉钼矿铼-钨同位素定年及其成矿意义 [J]. *岩矿测试*, 28(3): 265-268.